JOURNAL OF Applied Polymer SCIENCE

Synthesis, Characterization, and Self-Assembly of Amphiphilic Fluorinated Gradient Copolymer

Yanjun Chen, Yuying Zhang, Yifeng Wang, Chong Sun, Chaocan Zhang

Department of Polymer Materials and Engineering, School of Material Science and Engineering, Wuhan University of Technology, Wuhan 430070, China

Correspondence to: Y. Wang (E-mail: yifengwang@whut.edu.cn)

ABSTRACT: An amphiphilic copolymer of acrylic acid (AA) and 2,2,2-trifluoroethyl methacrylate (TFEMA) was synthesized by reversible addition-fragmentation transfer (RAFT) copolymerization, using a feed method for adding TFEMA. The kinetics of the RAFT copolymerization agreed well with those characteristic of a first-order reaction and the molecular weight of copolymers increased with the conversion increasing, both demonstrating that it proceeded in a controlled polymerization manner. Optimal copolymerization was achieved when the reaction was conducted at 70°C, using a molar ratio of TFEMA : AA : RAFT agent : initiator of 400 : 400 : 4 : 1. Analysis of instantaneous ^{1}H-NMR results proved that the obtained copolymer had a chain structure with AA segments gradually changing to TFEMA segments. The copolymer films had lower surface free energies and slightly microphase separation structures. The amphiphilic copolymer with gradient structures could self-assemble to form aggregates in selective solvents. The type and composition of solvent mixtures had great effects on the morphology and sizes of aggregates, which were investigated by transmission electron microscopy and dynamic light scattering, respectively. © 2012 Wiley Periodicals, Inc. J. Appl. Polym. Sci. 000: 000–000, 2012

KEYWORDS: amphiphilic fluorinated copolymer; gradient copolymer; RAFT; self-assembly

Received 15 December 2011; accepted 22 February 2012; published online
DOI: 10.1002/app.37556

INTRODUCTION

Fluorinated polymers containing perfluoroalkyl side chains have increasingly attracted the attention of many investigators because of their extraordinary properties (such as water-/oil-repellence) and wide-range applications, especially as surface coatings for textile, paper, and leather. Reported research work has focused mainly on the low surface energy of fluorinated materials.[1–4] A few observations on the self-assembly of amphiphilic fluorinated polymers indicate their potential applications for proton-conducting polymer membranes and delivery vehicles for highly hydrophobic particles.[5,6]

Gradient copolymer is a novel kind of copolymer, which has a composition that continuously changes from A comonomer unit to B comonomer unit along the molecular chain. Gradient copolymers exhibit unique properties[7,8] and interfacial behaviors,[9,10] which endows them with great potential applications in many fields,[11–13] such as compatibilizers in copolymer blends, damping materials, and biocompatible materials. Controlled radical polymerization technologies are suitable method to synthesize gradient copolymers, including atom transfer radical polymerization (ATPR),[14] nitroxide-mediated polymerization (NMP),[15] and reversible addition-fragmentation transfer (RAFT).[16] ATRP focuses on gradient copolymers of styrene–acrylates and methyl methacrylate–acrylates. NMP always are used to synthesize gradient copolymers of styrene with 4-hydroxystyrene, 4-acetoxystyrene, butadiene, chloromethylstyrene, acrylonitrile, methyl methacrylate, 2-hydroxyethyl methacrylate, 4-(hydroxymethyl)styrene, vinylpyrrolidone, and maleic anhydride. RAFT is a very reliable method to prepare gradient copolymers because of the versatility of monomers as well as the wide tolerance of reaction conditions.[17]

Amphiphilic copolymers can self-assemble to form aggregates with various specific morphologies in selective solvents, such as spheres, rods, lamellae, vesicles, micelles, hexagonally packed hollow hoops, and other complicated or inverted structures.[18,19] Compared with other kinds of amphiphilic copolymers, the self-assembly behavior of amphiphilic gradient copolymers exhibit some special characteristics.[20,21] Hoogenboom et al.[22] reported that gradient copolymers of 2-nonyl-2-oxazoline and 2-phenyl-2-oxazolin underwent significant structural changes in ethanol–

water solvent mixtures when the temperature or solvent composition changed. Okabe et al.[23] compared the self-assembly behavior of gradient copolymer of 2-ethoxyethyl vinyl ether and 2-methoxyethyl vinyl ether with that of their block copolymer and found that the microdomain structure formed by the gradient copolymer was less ordered than that of block counterpart due to the gradient chemical composition along the polymer chain. Therefore, it is of fundamental importance to explore the self-assembly behavior of amphiphilic gradient copolymers in selective solvents. However, the large van der Waals volume of fluorinated chains and low polarizability of fluorine make the fluorinated segments very hydrophobic, and thus the aggregates that fluorinated molecules form are quite stable.[5,24] It is worth noting that amphiphilic fluorinated copolymers with gradient structures have seldom been studied,[25] not only with respect to their self-assembly behavior, but also their synthesis technology.

Therefore, this work focuses on the synthesis of amphiphilic fluorinated gradient copolymers, their surface properties, and self-assembly behaviors. The amphiphilic gradient copolymer of acrylic acid (AA) and 2,2,2-trifluoroethyl methacrylate (TFEMA) were synthesized by RAFT solution polymerization with working in feed conditions. The RAFT polymerization conditions and kinetics were discussed in detail. The chemical structure, glass-transition temperature (T_g) and surface microtopography of the gradient copolymer were characterized by ^{1}H-NMR, FTIR, DSC, and AFM, respectively. Moreover, the self-assembly behavior of the obtained amphiphilic gradient copolymers in selective solvents was systemically investigated. The size and morphology of aggregates were studied by DLS and TEM, respectively.

EXPERIMENTAL

Materials and Pretreatment

TFEMA were obtained from Xuejia Chemical Reagents Company (Harbin, China) and used without further purification. AA and 1,4-dioxane were distilled under reduced pressure before use. AIBN was purified by recrystallization from methanol. RAFT reagent, 2-{[(dodecylsulfanyl) carbonothioyl] sulfanyl}propanoic acid, was synthesized according to the reported method[19] and recrystallized by using light petroleum and hexane. Other reagents and solvents were commercially available in the analytical grade and were used without further purification.

Characterization

The glass-transition temperature (T_g) of the synthesized gradient copolymer was measured using a heating rate of 5°C/min under a nitrogen atmosphere by TA-Q10 differential scanning calorimeter (TA Co). FTIR spectra of the copolymer were characterized by Nicolet NEXUS FTIR Spectrum (Thermo Nicolet Co). The chemical structures of the copolymers were confirmed by a Varian 400 MHz ^{1}H-NMR using dimethylsulfoxide-d_6 (DMSO-d_6) as the solvent. The sizes and morphologies of aggregates were studied by Nano-10 Series dynamic light scattering (DLS, Malvern instruments) and transmission electron microscope (TEM, JEOL, Japan), respectively. The microtopography of copolymer films were measured by Nanoscope IV Tapping mode atomic force microscope (AFM, Veeco) at room temperature. Contact angles of copolymer films were measured by the sessile drop method[26] at room temperature, using a JC2000A contact angle goniometer (Shanghai Zhongchen Powereach, China). Typically, three drops of liquid were placed on the surface of copolymer films and three readings of contact angles were taken for each drop. The average of nine readings was used as the final contact angle of each sample. Wetting liquids used for contact measurements were water and diiodomethane. The surface free energies of the films were calculated using Owens–Wendt surface energy' equation.[27]

$$\gamma_i(1+\cos\,\theta) = 2[(\gamma_i^d\gamma_s^d)^{1/2} + (\gamma_i^p\gamma_s^p)^{1/2}] \quad (1)$$

where γ_i is the surface tension of wetting liquid and γ_i^d and γ_i^p are the dispersive and polar components, respectively. γ_s^d and γ_s^p for copolymer films can be calculated by substituting values for water and diiodomethane into eq. (1) and solving the corresponding set of simultaneous equations. The total surface energy γ is the summation of γ_s^d and γ_s^p.

Polymerization of Gradient Copolymers

RAFT agent, AIBN, 2.88 g AA (0.04 mol), and 22.4 g 1,4-dioxane were added into a three-necked flask and mixed with stirring under nitrogen atmosphere. When reaction solution in the flask was heated to 70°C by water bath, 6.72 g TFEMA (0.04 mol) began to feed into the reaction system, using a microsyringe pump to maintain a feed rate of 0.1 mmol/min. The polymerization continued for 8 h. The product was precipitated from a hexane : ethanol mixture (20 : 1 by volume). The precipitate was then filtrated and dried in vacuum. The instantaneous conversions of RAFT copolymerization and components of the copolymers were respectively analyzed by gravimetric analysis and ^{1}H-NMR at a given time during the copolymerization. The copolymerization conditions and conversions are listed in Table I.

Self-Assembly of Gradient Copolymers in Selective Solvent

Gradient copolymers were dissolved in solvent mixtures (THF : H_2O or Dioxane : H_2O = 94 : 6, volume ratio) with a mechanical stirrer over 12 h. Distilled water was then added slowly (2 g/min) with vigorous stirring until the desired water concentration was reached (e.g., 20, 30, and 90%). The micellar solution with 90% water concentration was dialyzed for 3 days with deionized water, refreshed at an interval no longer than 8 h. The pore size of dialysis tubing was 2000 MWCO, obtained from Sigma.

RESULTS AND DISCUSSION

Effects of Polymerization Conditions on RAFT Copolymerization

To approach the aim that the copolymer would have a gradient molecular chain, RAFT technology was adopted. Using the Q-e value,[28,29] the reactivity ratio of AA and TFEMA was calculated, with r_{AA} = 0.80 and r_{TFEMA} = 0.85. Due to the close reactivity ratio of the two comonomers, a feeding method seemed most suitable. Moreover, using the feeding method would help to create a significant composition gradient along the chain. Our previous experimental efforts in synthesizing P(AA-block-TFEMA) indicated that it was easier for AA segments to transfer to TFEMA

Table I. Polymerization Conditions, Conversions, and T_g of Prepared Copolymers

Sample	RAFT agent (mmol)	AIBN (mmol)	Temperature (°C)	Conversion (wt %)	T_g (°C)
S-1	0.4	0.08	70	38.8	79.7
S-2	0.4	0.1	70	78.7	81.5
S-3	0.4	0.15	70	79.2	78.4
S-4	0.4	0.2	70	81.2	80.7
S-5	0.4	0.4	70	75.5	82.1
S-6	0.6	0.1	70	66.7	77.3
S-7	0.5	0.1	70	85.3	82.1
S-8	0.2	0.1	70	49.7	69.8
S-9	0.4	0.1	60	54.2	70.3
S-10	0.4	0.1	80	74.2	77.1

segments, rather than the reverse. Therefore, it was decided to feed TFEMA during the RAFT copolymerization reaction.

Figure 1 shows curves of conversion vs. reaction time along with kinetic plots for RAFT copolymerization of AA and TFEMA using different amounts of AIBN and RAFT agent. As anticipated from typical characteristics of living/control radical polymerization,[30] the kinetics would appear to be first order. Note that in the figure, the monomer polymerization rate $\ln[M_0]/[M]$ was rewritten in terms of conversion, X, and thus plotted as $\ln[1/(1-X)]$.

Comparing the kinetics plots S-1 through S-5, the effect of the amount of AIBN on the polymerization rate was distinct. The greater the amount of AIBN, the faster the polymerization rate. Additionally, however, the linear relationship in the kinetic plots became worse, indicating the controllability of the copolymerization became poorer. With increasing the amount of AIBN, the concentration of free radicals was increased. This led to more monomers being initiated, which resulted in faster polymerization, but less polymerization of controllability. When using a molar ratio of AA : TFEMA : RAFT : AIBN of 400 : 400 : 4 : 1, both the rate and final conversion of the copolymerization increased, moreover the kinetic plot maintained its linear relationship. Therefore, the optimal amount of AIBN was 1.0 mmol per 22.4 g 1,4-dioxane.

Using the optimal amount of AIBN, the effects of the molar ratio of RAFT to AIBN were further studied. Comparing the kinetic plots of S-2 with those of S-6, S-7, and S-8 in Figure 1, it could be seen that copolymerization was better controlled when the molar ratio of RAFT : AIBN was increased, although the copolymerization rate became slower. More dormant species formed via the reversible addition and fragmentation mechanism at a higher concentration of RAFT agent, which reduced the concentration of free radicals and in turn slowed down the copolymerization rate. When the ratio of RAFT : AIBN was 2 : 1, the copolymerization kinetics was not well fit with a linear relationship. When the molar ratio of RAFT : AIBN was 4 : 1, the copolymerization was well controlled and had the highest conversion.

Figure 2 shows the curves of conversion versus reaction time and the kinetics plots for the RAFT copolymerization of AA and TFEMA at 60, 70, and 80°C. The controllability of the copolymerization was strongly dependent on the reaction temperature. The higher the reaction temperature, the faster the polymerization rate in the early stages of polymerization. However,

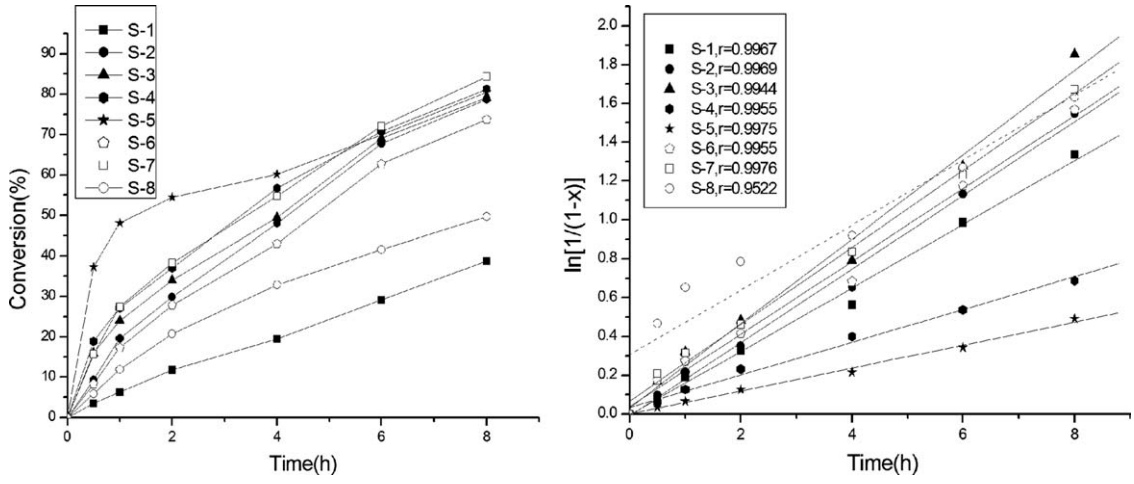

Figure 1. Curves of conversion versus reaction time (left) and kinetic plots (right) of RAFT copolymerization under different amounts of AIBN or RAFT agent. (x was conversion).

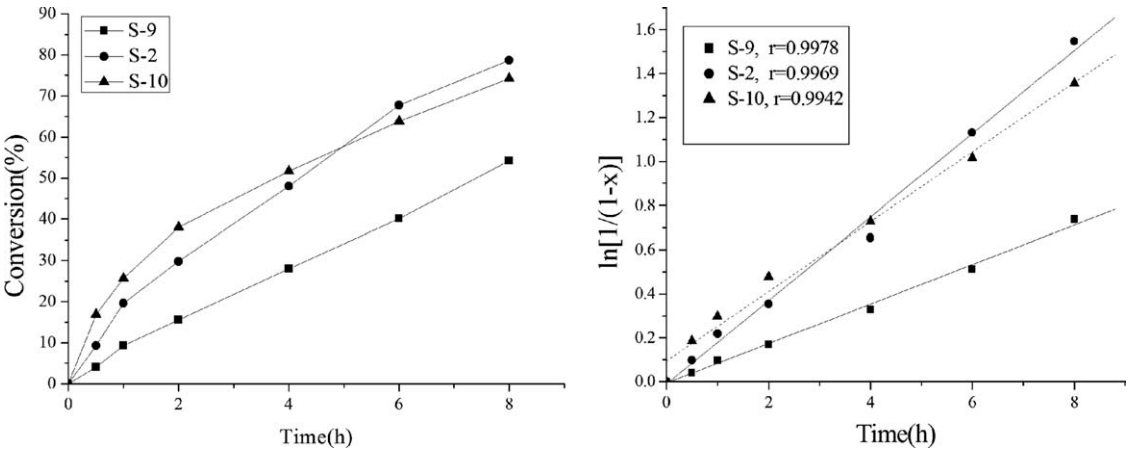

Figure 2. Curves of conversion versus reaction time (left) and kinetic plots (right) of RAFT copolymerization under different reaction temperatures. ([TFEMA] : [AA] : [RAFT] : [AIBN] = 400 : 400 : 4 : 1) (x was conversion).

the polymerization kinetics showed a worse linear relationship at higher temperature, with the polymerization kinetics at 80°C (S-10) deviating greatly from a linear relationship after 2 h. Under 70°C, both high final conversion and good polymerization controllability were achieved, therefore 70°C was the optimal reaction temperature.

Table II lists the copolymerization rate constants, as calculated using the slopes of the first-order kinetic plots within 2 h in Figure 2. From the Arrhenius equation, the activation energy for the reaction was calculated as 48.5 kJ/mol (with a linear correlation coefficient of fitting k to reaction temperature = 0.988).

Thus, the optimal conditions for RAFT copolymerization were found to be 70°C, with a molar ratio of AA : TFEMA : RAFT : AIBN of 400 : 400 : 4 : 1.

Chemical Structure of Copolymer

As shown in Figure 3, the wide absorption peak near 3000 cm^{-1} was evidence of —COOH group. The strong absorption at 1285 cm^{-1} was assigned to —CF_3 group. A strong and well-isolated band at 1710 cm^{-1} was due to the C=O stretching vibration of the ester carbonyl groups. The characteristic absorption peak for RAFT agent occurred at 1033 cm^{-1}, attributed to the stretching vibration of —C=S group. From DSC curve of P(AA-*grad*-TFEMA) showed in Figure 4, it was found that there was only one transfer region near 82.3°C, which was between the glass-transition temperature of the two monomer homopolymers (T_g of PAA = 102°C, and T_g of PTFEMA = 78.2°C). The results of FTIR and DCS both indicated that the obtained copolymer was composed of AA and TFEMA.

Table II. Reaction Rate Constants for RAFT Copolymerization of TFEMA and AA Under Different Temperatures

Reaction temperature (°C)	k (L/mol/s)
60	0.0856
70	0.1777
80	0.2310

Figure 5 shows ^{1}H-NMR spectra for the obtained P(AA-*grad*-TFEMA) copolymer under optimal polymerization conditions. The instantaneous compositions were determined from the ^{1}H-NMR peak areas observed at 12.2–12.4 ppm (—COO**H**, 1H), 4.3–4.7 ppm (—C**H**$_2$CF$_3$, 2H), and 0.85–0.87 ppm [—(CH$_2$)$_{11}$C**H**$_3$, 3H]. The instantaneous composition of each monomer unit in P(AA-*grad*-TFEMA) was calculated from the peak areas of the protons in AA unit and TFEMA unit using Kotani's method,[18] as listed in Table III.

$$F_A = \frac{A_1}{A_1 + A_2/2} = \frac{2A_1}{2A_1 + A_2} \quad (2)$$

where, A_1 and A_2 are peak areas of the protons in —COOH and —CH_2CF_3 group, respectively. F_A is instantaneous composition of AA in P(AA-*grad*-TFEMA). F_T is instantaneous composition of TFEMA = 1 − F_A.

Because of the low solubility of AA segment in THF,[16] the number average molecular weight (M_n) determined by GPC was a

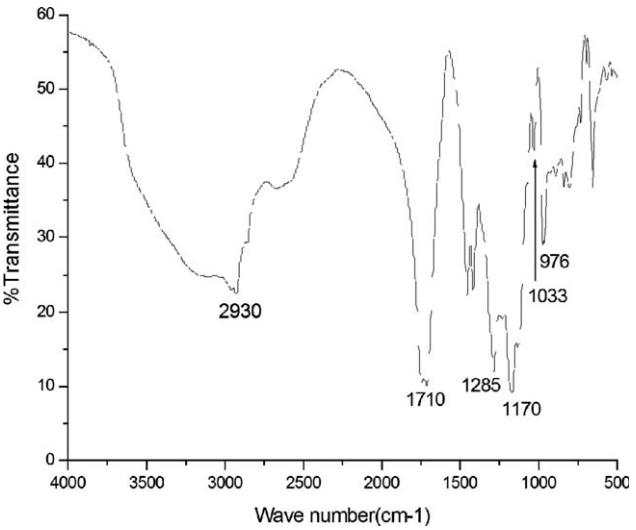

Figure 3. FTIR spectrum of P(AA-*grad*-TFEMA).

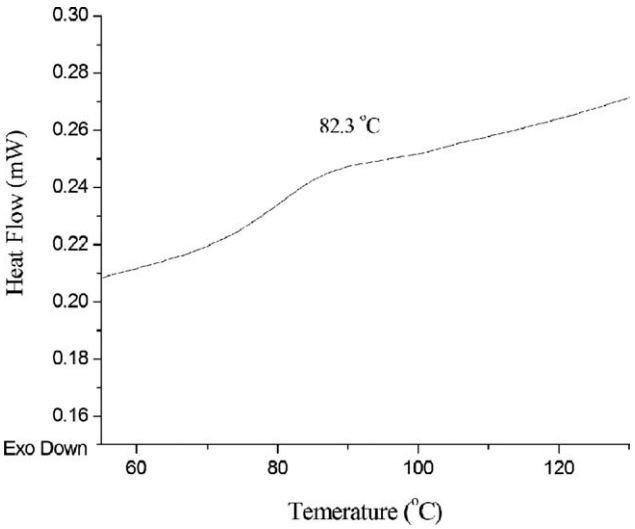

Figure 4. DSC curve of P(AA-*grad*-TFEMA).

larger apparent molecular weight of copolymer's aggregation. Therefore, molecular weights of P(AA-*grad*-TFEMA) in Table III were calculated from ^{1}H-NMR results. The molecular weight increased with the conversion increasing, which agreed well with the characteristic of controlled radical polymerization. At the same time, the instantaneous composition of AA unit in P(AA-*grad*-TFEMA) decreased, while that of TFEMA unit increased, indicating that the synthesized copolymer had a gradient composition change along the molecular chain from AA-rich at one end to TFEMA-rich at the other end. It was worth noticing that this gradient structure was within and along a molecular chain, which was great different from the gradient structures along the direction across the thickness of blend films we prepared before.[31,32]

Surface Free Energy and Morphology of P(AA-*grad*-TFEMA) Film

P(TFEMA-*grad*-AA) solution formed films at 70°C on cleaned glass slides. Contact angles and surface free energies of P(TFEMA-*grad*-AA) films are listed in Table IV. It was also worth noticing that the molar ratio of highly hydrophilic AA unit in copolymer chain was very high, even reaching 74% (in S-2), however, water contact angles of most P(AA-*grad*-TFEMA) films were close to 90°, even higher, indicating that these films could not be wetted by water easily. From the contact angles of water and diiodomethane, the surface free energies of the films were calculated using eq. (1), which were between the surface free energies of PTFEMA's film and PAA's. Because of the high hydrophobic character and low surface tension of perfluoroalkyl groups, TFEMA segments accumulated on the interface of the film and air during film formation, greatly decreasing its surface energy.[33]

Figure 6 displays the AFM images for the films of S-2 and S-7, which formed under 70°C. In Figure 6, a slight micro-phase separation was clearly observed in S-2's film, although not significantly in S-7's. It was likely the vastly different intrinsic properties of TFEMA and AA segments that caused the phase separation. However, the gradient chain structure of gradient copolymers had special interfacial properties.[34] Therefore, the gradient segments would be compatibilizers to AA segment and TFEMA segment, in turn, the phase separation of P(TFEMA-*grad*-AA) was not obvious. From roughness analysis of AFM surface morphology, roughness degrees of the films of S-2 and S-7 were 8.246 and 1.784nm, respectively.

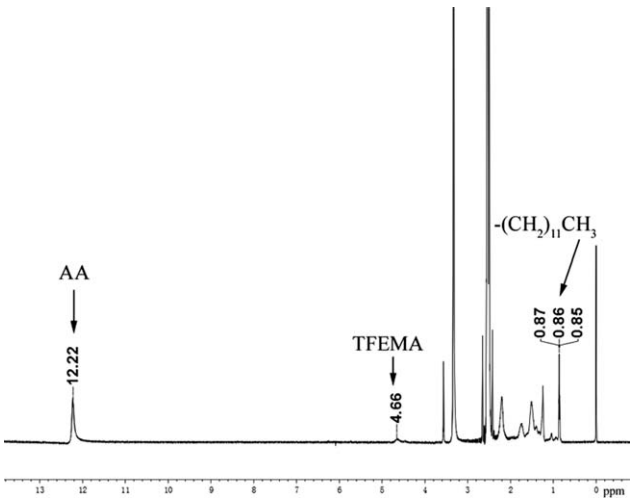

Figure 5. ^{1}H-NMR spectrum of P(AA-*grad*-TFEMA).

Table III. Absolute Molecular Weight and Instantaneous Composition of Each Monomer Unit in Copolymer Chain During Polymerization Progress

Reaction time (h)	1	2	4	8
Conversion (wt %)	13.8	31.5	53.9	81.2
Molecular weight (^{1}H-NMR)	1718	2775	3401	7342
F_A	1	0.97	0.87	0.74
F_T	0	0.03	0.13	0.26

Table IV. Contact Angles and Surface Free Energies of P(TFEMA-*grad*-AA) Films

Sample	Contact angles (°)		Surface energy (mN/m)
	Water	Oil	
S-1	84.5	49.0	35.78
S-2	95.0	59.3	29.13
S-3	93.2	58.0	29.88
S-4	81.3	44.3	38.56
S-5	86.0	50.2	34.89
S-6	85.0	53.2	33.68
S-7	87.0	49.9	33.47
S-8	84.1	52.3	30.17
PTFEMA	102.7	69.2	23.31
PAA	62.3	51.6	43.79

Applied Polymer SCIENCE

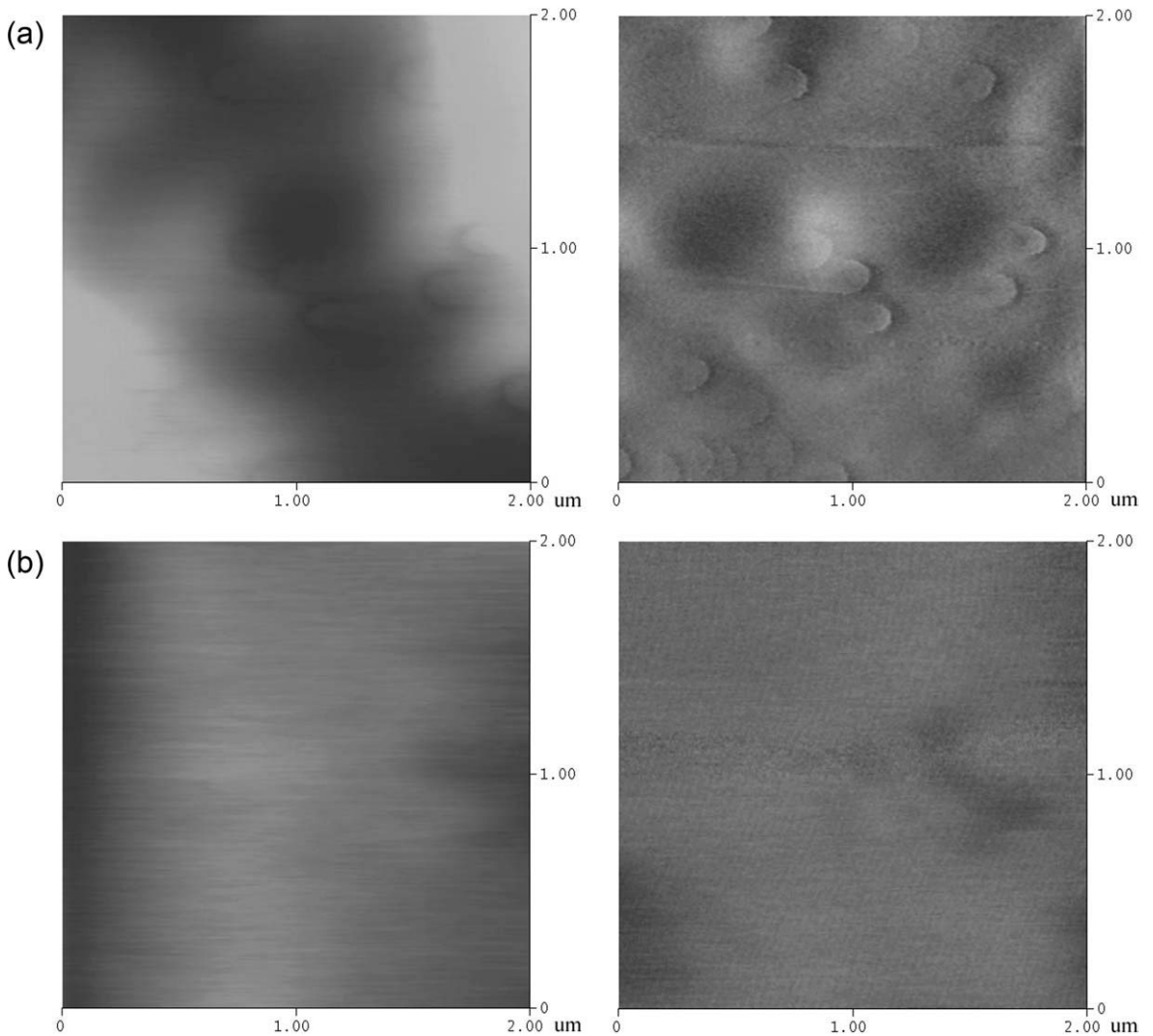

Figure 6. AFM surface morphology and phase graph of the film-air interface. (a: S-2; b: S-7).

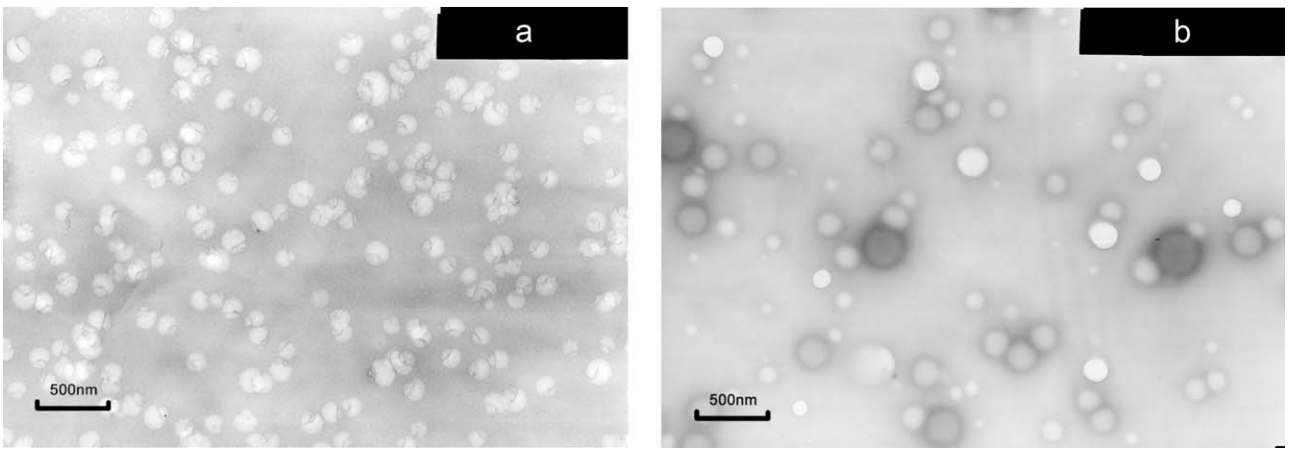

Figure 7. TEM morphology of micelles formed by S-2 with different molecular weights in different mixtures solvents. (90% water; a: THF–water; b: dioxane–water).

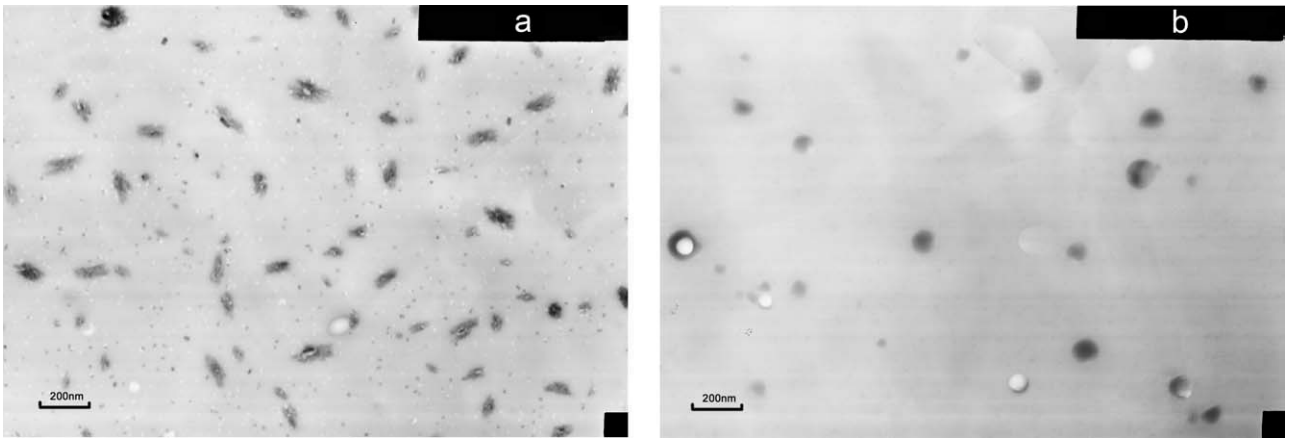

Figure 8. TEM morphology of micelles of S-2 in THF–water solution mixture with different water concentration. (a: 20% water; b: 30% water).

Self-Assembly of P(AA-*grad*-TFEMA)

Because of using a feeding method, P(AA-*grad*-TFEMA) chains contained both hydrophilic AA block segment and hydrophobic fluorinated block segment, thus exhibiting amphiphilicity. Because of noncovalent forces between solvent and the solute, such as van der Waals, electrostatic, and single-point hydrogen-bonding interactions, amphiphilic gradient copolymers could self-assemble into aggregates in selective solvents.[35] After nonsolvent (water) for TFEMA segment was added to the system, the amphiphilic P(AA-*grad*-TFEMA) molecules in solution mixture began to undergo microphase-separation. When the concentration of water reached a critical value, the self-assembly and phase segregation of TFEMA segments occurred, leading to the formation of micelles.

Figure 7 shows TEM photos of the micelles formed by S-2 in different solution mixtures (having induced the micelle formation by increasing the water : solvent ratio from 6 : 94 to 90 : 10, volume ratio). Tube-walled vesicles were observed in the THF–water mixture, while typical crew-cut micelles with core-shell structure formed in dioxane–water mixture. Moreover, the average sizes of micelles were larger in dioxane–water, which was also proven by DLS results (97 nm in THF–water, 164 nm in dioxane–water). This might arise from the different polarity index of the two solvents, leading to differences in the miscibility of each segment and giving the macromolecules different stretching capabilities in solutions. Therefore, their micelles exhibited different shapes and sizes.

It was found in Figure 8 that the morphology of S-2's micelles greatly depended on the concentration of water in the THF–water mixture. Therefore, two distinct kinds of micelles (spheres and rods) can be observed in Figure 8(a). DLS size analysis also showed a two-peak result and a larger DLS size distribution (PDI about 0.54). When the water concentration was 20%, some very small sphere micelles aggregated to form short-rod micelles. The reason for this possibility was that at 20% water concentration, the micelles lost their thermodynamic stability and as a result, the very small sphere micelles tried to minimize their free energies by aggregating and reconstructing into short rod micelles. As the water concentration increased to 30%, the rod-like structure lost their thermodynamic stability and thus a morphology transformation happened again, forcing the micelles to aggregate into the spherical structures shown in Figure 8(b).

CONCLUSIONS

Amphiphilic copolymers of AA and TFEMA were synthesized successfully using RAFT solution polymerization and a feed method of TFEMA. The results of the copolymerization showed good agreement with first-order kinetics, demonstrating that the copolymerization proceeded in a controlled manner. Optimal copolymerization was achieved when the reaction took place at 70°C, with a molar ratio of TFEMA : AA : RAFT agent : AIBN of 400 : 400 : 4 : 1. The results of FTIR, DSC, and ^{1}H-NMR proved that the amphiphilic copolymers of AA and TFEMA had a gradient component profile where each AA unit gradually transition to a TFEMA unit along the molecular chain. P(AA-*grad*-TFEMA) films had a lower surface free energy and slight microphase separation structures. The amphiphilic poly(AA-*grad*-TFEMA) could self-assemble in selective solvents to obtain crew-cut micelles with different ordered structures. The micellar morphology was significantly affected by the types of solvents and the concentration of water in mixed solvents.

ACKNOWLEDGMENTS

This research was supported by the National Natural Science Foundation of China (NSF) of China (No.50803048) and the Fundamental Research Funds for the Central Universities (No. 2010-Ia-009).

REFERENCES

1. Lin, Y. H.; Liao, K. H.; Chou, N. K.; Wang, S. S.; Chu, S. H.; Hsieh, K. H. *Euro. Polym. J.* **2008,** *44*, 2927.
2. Yao, L.; Yang, T. T.; Cheng, S. Y. *J. Appl. Polym. Sci.* **2010,** *115*, 3500.
3. Chen, Y. J.; Cheng, S. Y.; Wang, Y. F.; Zhang, C. C. *J. Appl. Polym. Sci.* **2006,** *99*, 107.
4. Casazza, E.; Mariani, A.; Ricco, L.; Russo, S. *Polymer* **2002,** *43*, 1207.

5. Hu, Z.; Verheijen, W.; Hofkens, J.; Jonas, A. M.; Gohy, J. F. *Langmuir* **2007,** *23*, 116.
6. Xu, S.; Liu. W. *J. Fluorine Chem.* **2008,** *129*, 125.
7. Buzin, A. I.; Pyda, M.; Costanzo, P.; Matyjaszewski, K.; Wunderlich, B. *Polymer* **2002,** *43*, 5563.
8. Mok, M. M.; Kim, J.; Torkelson, J. M. *J. Polym. Sci. Part B: Polym. Phys.* **2008,** *46*, 48.
9. Jiang, R.; Jin, Q. H.; Li, B. H.; Ding, D. T. *Macromolecules* **2008,** *41*, 5457.
10. Yuan, W.; Mok, M. M.; Kim, J.; Wong, C. L. H.; Dettmer, C. M.; Nguyen, S. T.; Torkelson, J. M.; Shull, K. R. *Langmuir* **2010,** *26*, 3261.
11. Tao, Y.; Kim, J.; Torkelson, J. M. *Polymer* **2006,** *47*, 6773.
12. Hashimoto, T.; Tsukahara, Y.; Tachi, K.; Kawai, H. *Macromolecules* **1983,** *16*, 648.
13. Lee, S. B.; Russell, A. J.; Matyjaszewski, K. *Biomacromolecules* **2003,** *4*, 1386.
14. Lee, H.; Matyjaszewski, K.; Sherryl, Y.; Sheiko, S. S. *Macromolecules* **2005,** *38*, 8264.
15. Kim, J.; Mok, M. M.; Sandoval, R. W.; Woo, D. J.; Torkelson, J. M. *Macromolecules* **2006,** *39*, 6152.
16. Ferguson, J. C.; Hughes, J. R.; Nguyen, D.; Pham, B. T. T.; Gilbert, R. G.; Serelis, K. A.; Such, H. C.; Hawkett, S. B. *Macromolecules* **2005,** *38*, 2191.
17. Moad, G.; Rizzardo, E.; Thang, S. H. *Aust. J. Chem.* **2006,** *59*, 669.
18. Kotani, Y.; Kamigaito, M.; Sawamoto, M. *Macromolecules* **1998,** *31*, 5582.
19. Zhou, J. H.Wang, L.; Ma, J. Z.; Wang, J. J.; Yu, H. J.; Xiao, A. G. *Euro. Polym. J.* **2010,** *46*, 1288.
20. Okabea, S.; Fusea, C.; Sugiharab, S.; Aoshimac, S.; Shibayama, M. *Physica. B* **2006,** *385–386*, 756.
21. Karaky, K.; Derail, C.; Reiter, G.; Billon, L. *Macromol. Symp.* **2008,** *267*, 31.
22. Hoogenboom, R.; Lambermont-Thijs, H. M. L.; Jochems, M. J. H. C.; Hoeppener, S.; Guerlain, C.; Fustin, C. A.; Gohy, J. F.; Schubert, U. S. *Soft Matter* **2009,** *5*, 3590.
23. Okabe, S.; Seno, K.; Kanaoka, S.; Aoshima, S.; Shibayama, M. *Polymer* **2006,** *47*, 7572.
24. Hoang, K.C.; Mecozzi, S. *Langmuir* **2004,** *20*, 7347.
25. Inoue, Y.; Watanabe, J.; Takai, M.; Yusa, S.-I.; Ishihara, K. *J. Polym. Sci. Part A: Polym. Chem.* **2005,** *43*, 6073.
26. Wu, S. *J. Colloid Interface Sci.* **1969,** *31*, 153.
27. Owens, D. K. *J. Appl. Polym. Sci* **1969,** *13*, 1741.
28. Zhao, X.; Sui, H.; Dong, Y.; Zhao, H.; Gao, D. *Shang Hai Coat* **2007,** *46*, 20.
29. Pan, Z., Eds. Polymer Chemistry; Chemical Industry Press: Beijing, **2003,** pp 95–96.
30. Yue, L.; Yuan, C.; Wang, Y.; Cao, T. *J. Chem. Eng. Chin. Univ.* **2005,** *19*, 654.
31. Hu, Y.; Zhang, C.; Chen, Y.; Liu, X.; Lv, M.; Hu, L. *Mater. Lett.* **2010,** *64*, 2091.
32. Hu, Y.; Zhang, C.; Chen, Y.; Hu, L.; Fan, Y. *Acta. Polym. Sinica.* **2011,838.**
33. Thomas, R. R.; Auton, D. R.; Graham, W. F. *Macromolecules* **1997,** *30*, 2883.
34. Wang, R.; Li, W.; Luo, Y.; Li, B.-G.; Shi, A.-C.; Zhu, S. *Macromolecules* **2009,** *42*, 2275.
35. Lobert, M.; Hoogenboom, R.; Fustin, C. A.; Gohy, J. F.; Schubert, U. S. *J. Polym. Sci. Part A: Polym. Chem.* **2008,** *46*, 5859.